Am J Stem Cells 2023;12(5):124-137
www.AJSC.us /ISSN:2160-4150/AJSC0154034

Original Article

Study on the protective effect of OM-MSCs on Golgi apparatus after intracerebral hemorrhage in Sprague-Dawley rats

Junjiang Liu[1], Zhiping Hu[2], Yan Huang[3,4,5], Yidan Zhang[6], Dezhen Peng[6]

[1]Department of Geriatrics, Hunan Provincial People's Hospital (First Affiliated Hospital of Hunan Normal University), No. 61 Jiefang West Road, Changsha 410011, Hunan, The People's Republic of China; [2]Department of Neurology, The Second Xiangya Hospital of Central South University, Changsha 410011, Hunan, The People's Republic of China; [3]Hunan Provincial Maternal and Child Health Care Hospital, Changsha 410008, Hunan, The People's Republic of China; [4]Key Laboratory of Protein Chemistry and Developmental Biology of Ministry of Education, College of Life Sciences, Hunan Normal University, Changsha 410081, Hunan, The People's Republic of China; [5]Hunan Provincial University Key Laboratory of The Fundamental and Clinical Research on Neurodegenerative Diseases, Changsha Medical University, Changsha 410219, Hunan, The People's Republic of China; [6]Clinical Nursing Teaching and Research Section, The Second Xiangya Hospital of Central South University, Changsha 410011, Hunan, The People's Republic of China

Received October 21, 2023; Accepted December 14, 2023; Epub December 15, 2023; Published December 30, 2023

Abstract: Introduction: The present study aimed to assess alterations in apoptosis rate, Golgi morphology and GOLPH3 expression following intracerebral hemorrhage (ICH) both before and after intervention with OM-MSCs. The objective was to investigate the impact of ICH on Golgi apparatus (GA) stress and to explore the potential protective effects of OM-MSCs on GA following ICH. Material and methods: A total of 54 Sprague-Dawley rats were allocated into three experimental groups: sham operation group, ICH group and OM-MSCs group. ICH models were established by collagenase method while OM-MSCs were cultured in vitro. In OM-MSCs intervention group, one million OM-MSCs were stereotactically injected into unilateral striatum of rats 48 hours after ICH modeling while other two groups received an equivalent volume of PBS. Brain tissues were collected at 1 day, 3 day and 7 day post intervention and subsequently assessed for cellular apoptosis, morphological change of GA and expression of GOLPH3. The obtained data were subjected to statistical analysis by SPSS 21.0. Results: 1. Apoptosis rate in the 1 d and 3 d ICH groups was significantly higher compared to sham operation group ($P < 0.05$), but significantly lower compared to OM-MSCs intervention group ($P < 0.05$). 2. While no noticeable morphological changes were observed in sham operation group, GA in ICH group exhibited a significant increase fragmentation. After OM-MSCs intervention, the fragmentation of GA decreased significantly. 3. On 3 d, expression of GOLPH3 in ICH group was significantly higher than that in sham operation group ($P < 0.05$) but significantly lower than that of OM-MSCs intervention group ($P < 0.05$). Conclusions: The rate of apoptosis, fragmentation of GA, and expression of GOLPH3 exhibited significant increases following ICH in SD rats. Conversely, all of these factors demonstrated significant decreases subsequent to early intervention with OM-MSCs, thereby exerting neuroprotective effects.

Keywords: Intracerebral hemorrhage, olfactory mucosa mesenchymal stem cells, GOLPH3, Golgi apparatus stress (GAS), apoptosis, neuroprotection

Introduction

Intracerebral hemorrhage (ICH) is defined as the primary non-traumatic intraparenchymal hemorrhage, constituting approximately 10-30% of all stroke cases globally [1, 2]. It is considered one of the most severe cerebrovascular diseases due to its high morbidity, mortality, and disability rates [3, 4]. The pathogenesis of acute ICH encompasses two main aspects: primary brain injury and secondary brain injury. Primary injury occurs within the first few hours after ICH and involves the mass effect of the hematoma as well as sequential mechanical damage to adjacent brain tissue. Secondary brain injury, which is initiated by the primary injury [5], involves a complex interplay of pathophysiological processes such as inflammation,

oxidative stress, blood-brain barrier disruption, and apoptosis pathways [6, 7]. These processes play a crucial role in exacerbating the disease and leading to further deterioration [8]. As a result, addressing secondary injury in the acute stage after ICH and enhancing the long-term prognosis of patients is a critical aspect of ICH treatment, among which oxidative stress is the key node.

Traditionally, mitochondria, the respiratory hub of cells, have been considered to play a major role in oxidative stress [9]. However, increasing studies have shown that oxidative stress is a comprehensive defense process. Mitochondria, lysosome and endoplasmic reticulum have been proved to be involved in oxidative stress injury induced by cerebral ischemia/reperfusion through their respective classical reactions [10]. Similarly, the homeostasis structure and physiological functions of Golgi apparatus (GA) are also affected in process of oxidative stress and undergo adaptive changes, collectively referred to as 'Golgi Apparatus stress (GAS)' [11]. GAS theory acknowledges that stress signal can be sensed by GA, triggering adaptive changes in structure and function including the activation of genes that encoding defensive enzymes, transcription factors and structural proteins resulting in self-restoration or, if the oxidative stress is too severe, GA fragmentation and even apoptosis [11]. GAS has been confirmed in cerebral ischemia/reperfusion models [12], suggesting a role in cellular stress response. Additionally, local circulation disorder, ischemia/hypoxia, and inflammatory responses after ICH occur in the perihematoma region, leading to speculation that GAS may also occur in cells adjacent to the hematoma and requires further investigation for verification.

Previous studies have confirmed that Golgi phosphphoprotein-3 (GOLPH3), known as the 'sensor' of GAS, is a stress-related protein of GA [12]. GOLPH3 is abundant in mammalian cells and is a new type of membrane protein mainly located in the trans Golgi network. It plays a pivotal role in maintaining the normal structure and physiological function of GA. When GOLPH3 is knocked out, GA loses tension and focuses on the lateral side of the nucleus. In vitro studies using an oxyglucose deprivation/reperfusion model have shown that the expression and location of GOLPH3 are directly related to GAS. GOLPH3 can rapidly transfer from GA to the cytoplasm in response to oxidative stress, providing a dynamic reflection of the level of oxidative stress in neurons. Moreover, under intense and continuous stress, elevated GOLPH3 can further induce GA fragmentation and activate downstream autophagy and apoptosis signals [13]. Therefore, measuring the expression of GOLPH3 could verify the existence of GAS after ICH and determine the intracellular stress level.

Although the pathophysiological mechanisms for brain injury after ICH have been well investigated and understood, the current focus of ICH treatment predominantly centers on mitigating primary mechanical injury and preventing secondary hemorrhage [14] and edema formation. Such interventions include surgical measures, dehydration, blood pressure control [15], infection prevention, and rehabilitation [16]. However, these strategies have shown limited curative efficacy [17, 18]. Consequently, there is an urgent clinical need to identify effective treatments capable of counteracting ICH-induced injuries. Mesenchymal stem cell (MSC) therapy has emerged as a promising treatment avenue with substantial potential for clinical implementation [19], sparking significant interest among researchers. Notably, a growing body of evidence in recent years has bolstered the understanding that the paracrine effect [20] plays a pivotal role in the therapeutic mechanism of MSCs, exerting anti-inflammatory, antioxidant, and anti-apoptotic effects [21-23].

Olfactory mesenchymal stem cells (OM-MSCs), also known as Olfactory ectomesenchymal stem cells (OE-MSCs) [24], derive their name from the region where they were initially discovered [25]. These cells are situated in the lamina propria of the olfactory mucosa [26] and originate from the ectoderm, the same origin as the nervous system. Additionally, they share similar biological characteristics with MSCs originating from the bone marrow, showing the ability to differentiate into nerve cells, osteoblasts, adipocytes, and other multidirectional cells under specific induction conditions [27]. OM-MSCs offer several advantages [28], including their superior proliferation efficiency, ease of collection from the nasal mucosa, potential for autol-

ogous transplantation with no risk of immune rejection, high safety with no gene mutation, and absence of ethical concerns. Consequently, they have become the ideal seed cells in tissue engineering [29, 30]. Currently, 274 secreted proteins have been identified in the secretome of OM-MSC, which play essential roles in neuronutrition, angiogenesis, cell growth and differentiation, apoptosis, and inflammation. These biological molecules are closely associated with central nervous system repair [22]. However, there is a dearth of relevant studies on the use of OM-MSCs in ICH models. Consequently, it remains unclear whether OM-MSCs could attenuate secondary brain injury after ICH through their antioxidant effect. Therefore, this study aims to comprehensively verify these assumptions and explore the protective effects of OM-MSCs on secondary brain injury after ICH in SD rats.

Material and methods

Acquisition of human OM-MSCs

The olfactory mucosa mesenchymal stem cells (OM-MSCs) were isolated and purified using the olfactory mucosa adherent method, as per the protocol described in the studies by Lite Ge et al. [27, 30]. Tissue blocks of olfactory mucosa were harvested from nasal-healthy volunteers after obtaining written informed consent and approval from the ethics committee of Hunan Normal University. The sampling area was approximately 2 cm^3 near the surface interior of the concha nasalis media, with the understanding that it would recover within one month without impacting olfactory function. The tissues underwent three rounds of decontamination washing with serum-free high-glucose Dulbecco's Modified Eagle Medium/Nutrient Mixture F-12 (DMEM/F-12; Invitrogen) and were then placed in a specific petri dish containing 10% fetal bovine serum (FBS; Invitrogen) medium DMEM/F-12. Following this, the tissues were cut into small 1 mm^3 pieces. The tissue blocks were then incubated in a Corning culture bottle at 37°C in 5% CO_2, with continuous monitoring of cell growth and medium change conducted every 3 days. Upon reaching 80% coverage of the culture bottle bottom, trypsin was used for cell digestion and passage. Cells that reached the 5th generation were collected for transplantation.

Animals

Healthy adult male Sprague-Dawley rats (average weight 250 g) were obtained from Slac Laboratory Animal Co., Ltd. (Shanghai, China). The animals were maintained under controlled temperature of approximately 25°C and humidity conditions of approximately 55% in a 12-hour light/dark cycle. All procedures involving animals strictly conformed to the Chinese legislations involving animal protection and were approved by the ethics committee of Hunan Normal University.

Experimental groups and OM-MSCs interventions

A total of 54 healthy male SD rats were randomly divided into three major groups: sham operation group, ICH group and OM-MSCs intervention group, each comprising 18 rats. Subsequently, each group was further categorized into subgroups based on varying observation times post-intervention: 1 d sham operation group, 3 d sham operation group, 7 d sham operation group, 1 d ICH group, 3 d ICH group, 7 d ICH group, 1 d OM-MSCs intervention group, 3 d OM-MSCs intervention group, and 7 d OM-MSCs intervention group, with 6 rats in each subgroup (n=6). The ICH model of SD rats was established using the collagenase method [30], while the sham operation group underwent stereotactic injection of an equivalent volume of sterile saline. In contrast, the OM-MSCs intervention group received a stereotaxic injection of OM-MSCs suspension 48 hours after the establishment of the ICH model, while the other two groups were injected with phosphate buffer solution (PBS) at the same time point. Subsequently, rats from all three groups were decapitated at 1 d, 3 d and 7 d after the intervention, to prepare specimens for further analysis.

ICH model

ICH model in rats was induced by collagenase type IV [31, 32]. 10% chloral hydrate (3 ml/kg) was used for intraperitoneal injection to anesthetize the rats. The animals were placed on the operation platform of rat brain stereotactic apparatus and under aseptic condition. Then, the skull and bregma were exposed by a midline incision on the scalp and a cranial burr hole with a diameter of 1 mm was drilled in the right

part of the brain. Target injection point was situated on the right striatum with coordinates 0.2 mm anterior and 3.0 mm lateral to bregma and 6.0 mm below the surface. A 10-μl microsyringe with a needle tip was inserted stereotactically through the burr hole and into the right striatum. Collagenase type IV (0.3 U in 2 μl sterile normal saline; Sigma-Aldrich, St. Louis, MO) was administered over a period of 10 min via stereotaxic intrastriatal injection. The needle was kept in situ after the injection for another 5 minutes before slow withdraw in case of backflow. The burr hole was sealed with medical bone wax and the scalp was sutured after disinfection. After the animals wake up (average time 2 hours), Zea Longa 5-grade scale [33] was used to determine whether the modeling was successful. When neurological deficits of rats was more than 2 points, the model was considered to be successful. Those who died, had subarachnoid hemorrhage or scored less than 2 points were excluded from the experiment.

Transplantation of OM-MSCs

Stereotactic intracerebral transplantation was administrated in this study [34, 35]. 48 hours after establishment of ICH model, rats in OM-MSCs intervention group was anesthetized and undergone same procedure of ICH modeling except the part where 10-μl OM-MSCs suspension (1×10^6 OM-MSCs) was injected slowly by microsyringe at a speed of 1 ul/min though the original burr hole reaching depth 5.0 mm below the surface. Rats in sham operation group and ICH group were injected with equivalent amount of PBS at the same site.

Preparation of paraffin-embedded sections

After abdominal anesthesia with 10% chloral hydrate (3 ml/kg), the rats were swiftly decapitated and their brains were immediately immersed with 4% paraformaldehyde solution and postfixed at 4°C for at least 24 hours. After dehydration and vitrification, tissue samples were embedded in paraffin, and 5-μm sections were prepared. The sections were then dewaxed in xylene, rehydrated in graded ethanol and deionized water, and then processed for hematoxylin & eosin staining, TdT-mediated dUTP Nick-End Labeling (TUNEL) staining and immunofluorescence.

Hematoxylin and eosin staining

Coronal brain sections (5 μm thickness, paraffin embedded) were prepared as mentioned above and next stained with eosin for 10 seconds followed by hematoxylin restaining for 5 minutes. After dehydrated in graded ethanol and cleared in xylene, slides were mounted by neutral balsam. Images were obtained by the usage of a microscope (Olympus, Tokyo, Japan).

TUNEL staining

Coronal paraffin-embedded 5 μm thickness brain sections were prepared as mentioned above, and apoptotic cells were determined with TUNEL staining using TUNEL Apoptosis Detection Kit (Yeasen Biotech Co., Ltd.) as indicated in the manufacturer's instructions. The number of TUNEL-positive cells was determined at high magnification (×400 magnification) and was measured in eight hemorrhage boundary zones in four different slices of the ipsilateral hemisphere for each animal. It was also counted and analyzed by two investigators blinded to the grouping.

Immunofluorescence staining

Coronal paraffin-embedded sections were prepared as described previously. Briefly, after dewaxing and hydration procedures, brain sections were heated in a microwave oven for 25 minutes in ethylene diamine tetra-acetic acid (EDTA) buffer solution (pH 9.0) for antigen retrieval and blocked by 5% bovine serum albumin (BSA) for 60 minutes. Then, sections were incubated overnight at 4°C with primary antibodies: anti-GM130 (610822, 1:100, BD, USA) and anti-GOLPH3 (ab98023, 1:50, Abcam, Cambridge, MA), and with appropriate secondary antibodies for 90 minutes at room temperature in the dark. Next, the sections were rinsed and stained with 4',6-diamidino-2-phenylindole (DAPI) for 10 minutes and mounted with glycerol. Changes of GA morphology were finally observed by using a fluorescence microscope (Motic, China).

Western blotting

Proteins for Western blot were harvested by radio-immunoprecipitation assay (RIPA) lysis buffer from brain tissues surrounding the hematoma. Detail procedures of Western blot

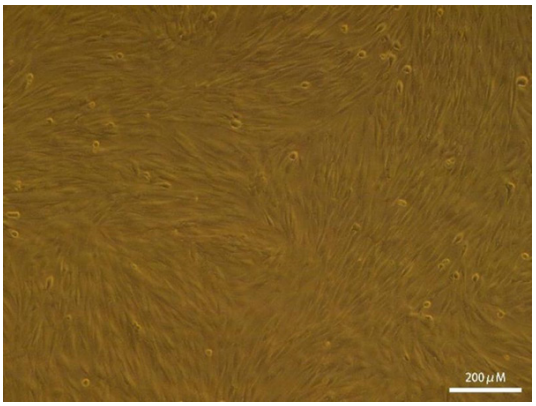

Figure 1. The 3rd generation OM-MSCs (×40). The morphology of OM-MSCs tended to show a typical parallel or swirling growth pattern.

were described previously [36, 37]. In short, proteins separated by sodium dodecyl sulfate polyacrylamide gel (SDS-PAGE) were transferred to nitrocellulose membranes in an electromagnetic field. Next, membranes were blocked by 5% nonfat milk in Phosphate-buffered saline-Tween 20 (PBST) for 90 minutes and probed at 4°C overnight with primary antibodies: anti-GOLPH3 (ab98023, 1 ug/ml, Abcam, Cambridge, MA) and β-actin (66009-1-Ig, 1:5000, Proteintech, USA) serving as the internal control. After undergoing repeated washes with PBST, membranes were incubated with secondary antibody under room temperature for 90 minutes. The protein band densities were detected using X-ray film and quantified using ImageJ software (National Institutes of Health, Baltimore, MD). To facilitate comparisons between the groups, the band density values were normalized to the mean value of the control group.

Quantitative and statistical analysis

For quantitation, fragmented Golgi was defined as scattered dots (not connected) in the perinuclear region or multiple mini-Golgi (isolated dots) dissociated from the major GA [38, 39]. Quantification was performed using more than 300 cells per experiment. The experimental data were analyzed using SPSS21.0 software package, and each experiment was repeated for at least 3 times. Data were expressed as mean ± SEM and plots were drawn by GraphPad Prism 8 software (Graph-Pad Software, Inc., San Diego, CA). One-way analysis of variance followed by least significant difference tests was used to compare differences among multiple groups. If data were unequal, Dunnett's T3 tests were taken into consideration. Differences were determined as significant when $P < 0.05$.

Results

Survival of animals

Out of the initial 18 SD rats in the sham operation group, all 18 successfully survived. For the ICH modeling experiment, a total of 46 rats were initially involved, but 7 rats were later excluded due to either death, subarachnoid hemorrhage, or neurological deficits scores less than 2 points. From the remaining 39 rats, 18 were allocated to the ICH group. Additionally, out of the remaining 21 rats designated for the OM-MSCs intervention group, 3 were excluded due to mortality following intracerebral transplantation during the subsequent observation period.

Isolation and culture of OM-MSCs

After 1 day, the tissue blocks typically adhere to the wall, and the majority of cells migrate out within 7-8 days. The cells exhibit characteristic morphological features of mesenchymal stem cells (MSCs), such as elongated fusiform, spindle, or polygonal shapes. Upon culturing the primary cells for 14 days, they could achieve 80% confluence for passage. Following passage, the growth rate was enhanced, enabling passage approximately every 2-3 days, with the potential for over 10 passages. By the third generation, the cells demonstrated high purity and tended to exhibit consistent morphology, characterized by typical parallel or swirling growth arrangement of MSCs (**Figure 1**). Subsequent transmission to the fifth generation yielded highly pure OM-MSCs.

OM-MSCs ameliorate brain tissue swelling and inflammatory infiltration after ICH by intracerebral administration

The histopathological morphology around the hematoma following ICH in SD rats was observed using HE staining and a light microscope (**Figure 2**). The tissue structure of the right striatum, corresponding to the hematoma area of the ICH group in the sham operation group, exhibited complete integrity with normal

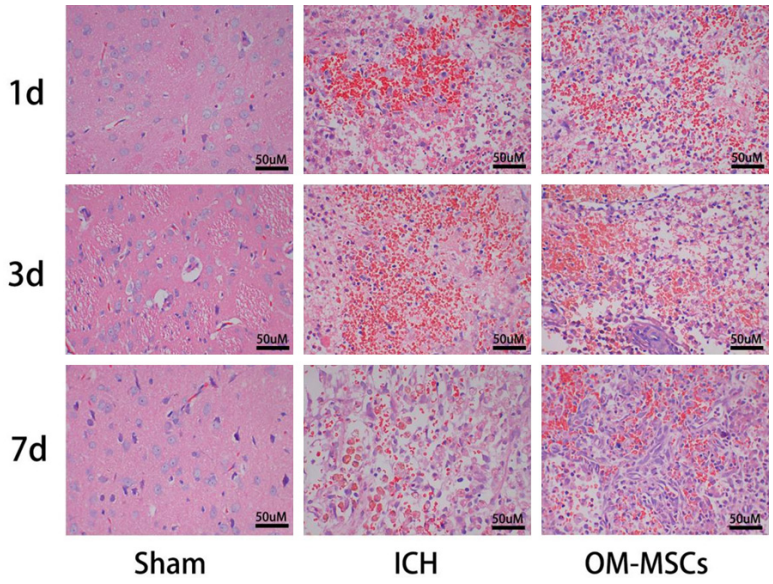

Figure 2. Hematoxylin and eosin staining in three groups at different time points. Sham: sham operation group, ICH: ICH group, OM-MSCs intervention group. Compared with sham operation group, bleeding foci and diffuse distribution of red blood cells, swelling of neurons and glial cells, fuzzy nuclear structure and necrosis of some nuclei were visible accompanied by inflammatory cell infiltration in ICH group. After OM-MSCs administration, tissue swelling, inflammatory infiltration and integrity of structure were improved obviously, accompanied by glial cell proliferation.

neurons and glial cells visible. No significant differences were observed at different time points, and there was no evidence of inflammatory cell infiltration. However, in the ICH group, bleeding foci and diffuse distribution of red blood cells were apparent, along with neuronal and glial cell swelling, fuzzy nuclear structure, necrosis of some nuclei, widened cell and perivascular space, tissue loosening and swelling, and significant inflammatory cell infiltration. Conversely, in the OM-MSCs intervention group, an improvement in the perihematoma area was observed with reduced tissue swelling and inflammatory infiltration, as well as structural integrity and enhanced glial cell proliferation in comparison to the ICH group.

OM-MSCs stereotactic transplantation decreased apoptosis rate after ICH

The effects of OM-MSCs transplantation after ICH were investigated by detecting cell apoptosis using the TUNEL Apoptosis Detection Kit in the ICH rat model. **Figure 3** illustrates that the ICH group exhibited a higher number of TUNEL-positive cells and a significantly increased cell apoptotic rate in the perihematomal area on 1 d and 3 d, compared with the sham operation group ($P < 0.05$ vs. sham). Notably, the intervention with OM-MSCs resulted in a reduced number of TUNEL-positive cells, and the cell apoptotic rate was significantly downregulated in the perihematomal area on 1 d and 3 d, compared with the ICH group ($P < 0.05$ vs. ICH).

OM-MSCs reduced GA fragmentation after ICH by stereotactic administration

In this study, GA morphology was examined using immunofluorescence confocal observation of GOLPH3 and the GA specific marker protein-GM130 (**Figure 4**). Significant fragmentation of GA was observed in the ICH group in comparison with the sham operation group in the brain tissue adjacent to the hematoma at 1 d, 3 d, and 7 d. Conversely, in the OM-MSCs intervention group, the structure of GA was visibly maintained, and GA fragmentation was significantly reduced compared with the ICH group around the bleeding area at 1 d and 3 d. It was noteworthy that the green fluorescence of the GA stress protein GOLPH3 and the red fluorescence of the GA specific marker protein GM130 were clearly overlapped in each group. These findings collectively indicate that GOLPH3 plays a role in GA stress and contributes to maintaining the structure of GA in the secondary brain injury following ICH.

OM-MSCs administration decreased expression of GOLPH3 after ICH

GOLPH3, a stress-related protein of GA, is known to play a crucial role in GAS. Western blot analysis (**Figure 5**) demonstrated a significant upregulation of GOLPH3 expression at 3 d and 7 d post-ICH compared to the Sham group ($P < 0.05$ vs. Sham). Remarkably, administration of OM-MSCs resulted in a notable inhibition of the ICH-induced upregulation of GOLPH3 on the 3rd day ($P < 0.05$ vs. ICH), suggesting the involvement of GAS in this process.

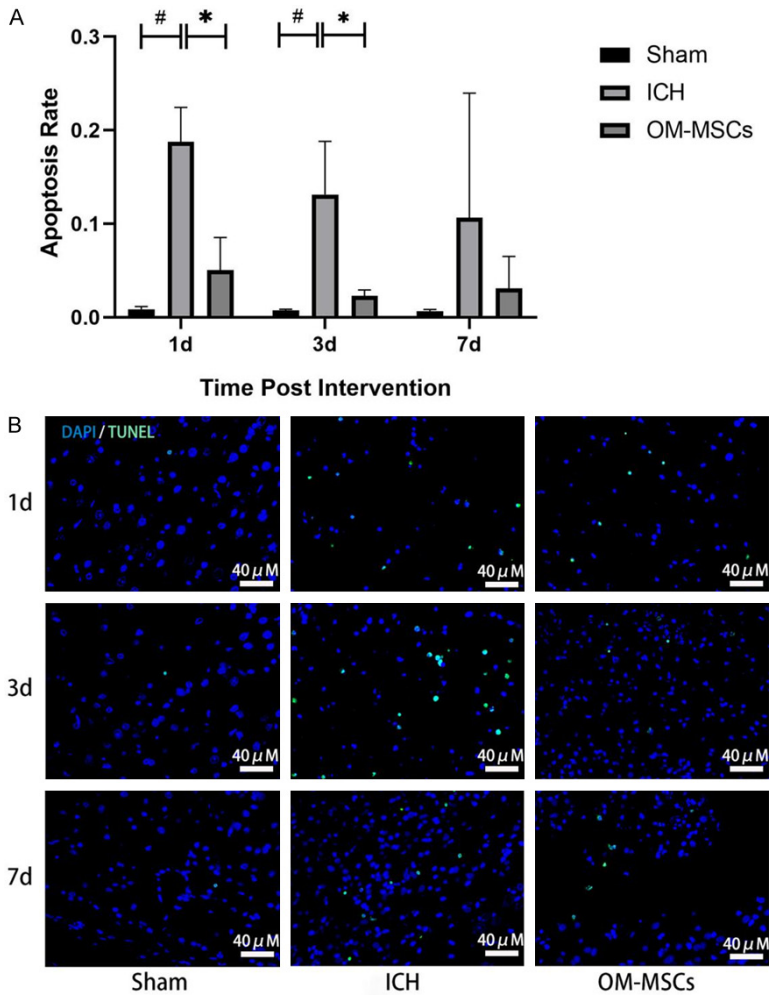

Figure 3. Apoptosis rate (A) and TUNEL staining (B) in three groups at different time points. ICH group exhibited an increased number of TUNEL-positive cells and cell apoptotic rate was significantly upregulated compared with sham operation group on 1 d, 3 d. OM-MSCs intervention demonstrated a decreased number of TUNEL-positive cells and cell apoptotic rate was significantly down-regulated compared with ICH group on 1 d, 3 d. Sham: sham operation group, ICH: ICH group, OM-MSCs intervention group. #P < 0.05 ICH versus Sham, *P < 0.05 OM-MSCs versus ICH. Representative microphotographs displayed the colocalization of DAPI (blue) with TUNEL (green) positive cells in the perihematomal areas. DAPI: 4'6-diamidino-2-phenylindole, TUNEL: TdT-mediated dUTP Nick-End labeling.

Discussion

In this study, we conducted a preliminary investigation into the protective effect of OM-MSCs on GA in ICH rats. Our observations indicate that the stereotactic transplantation of OM-MSCs after ICH results in a significant protective impact, as evidenced by the decrease in apoptosis, reduction in GA fragmentation, and inhibition of GOLPH3 expression in the perihematomal areas. These findings represent a novel demonstration of the neuroprotective effects of OM-MSCs on GA in a rat ICH model. As such, our results suggest that OM-MSCs transplantation holds promise as a potential therapy for mitigating early brain injury following ICH.

Prior studies have demonstrated significant enhancement in the structure and function of the brain following ICH through the transplantation of various types of MSCs. However, the optimal administration time window, route, and dosage of OM-MSCs for therapy remain uncertain. This critical issue necessitates prioritized attention as it has substantial implications for successful treatment outcomes. Majority of scholars believe that MSCs transplantation should be performed early [40] after the occurrence of ICH to capitalize on its neuropretective effects [40-42] and to initiate the commencement of endogenous nerve restoration [43] as early as possible. Conversely, some scholars argue that the adverse effects of factors such as hemorrhage, toxic substances produced by cell necrosis, inflammation factors, and oxygenic free radicals during the acute phase may pose a hindrance to the survival and proliferation of transplanted cells [44, 45]. In this sense, appropriate delay of OM-MSCs transplantation was selected in acute period, namely 48 h [46] after ICH modeling in SD rats, in order to minimize adverse effects and exert expected impacts. The most common routes for successful transplantation of MSCs include intracerebral [34], intravenous [47], intra-arterial [48], intranasal [49], intraventricular [50] and intrathecal routes [51]. Among these, intravenous and intracerebral routes are widely used. The intravenous route is favored for its minimal invasiveness and straightforward procedure, making it

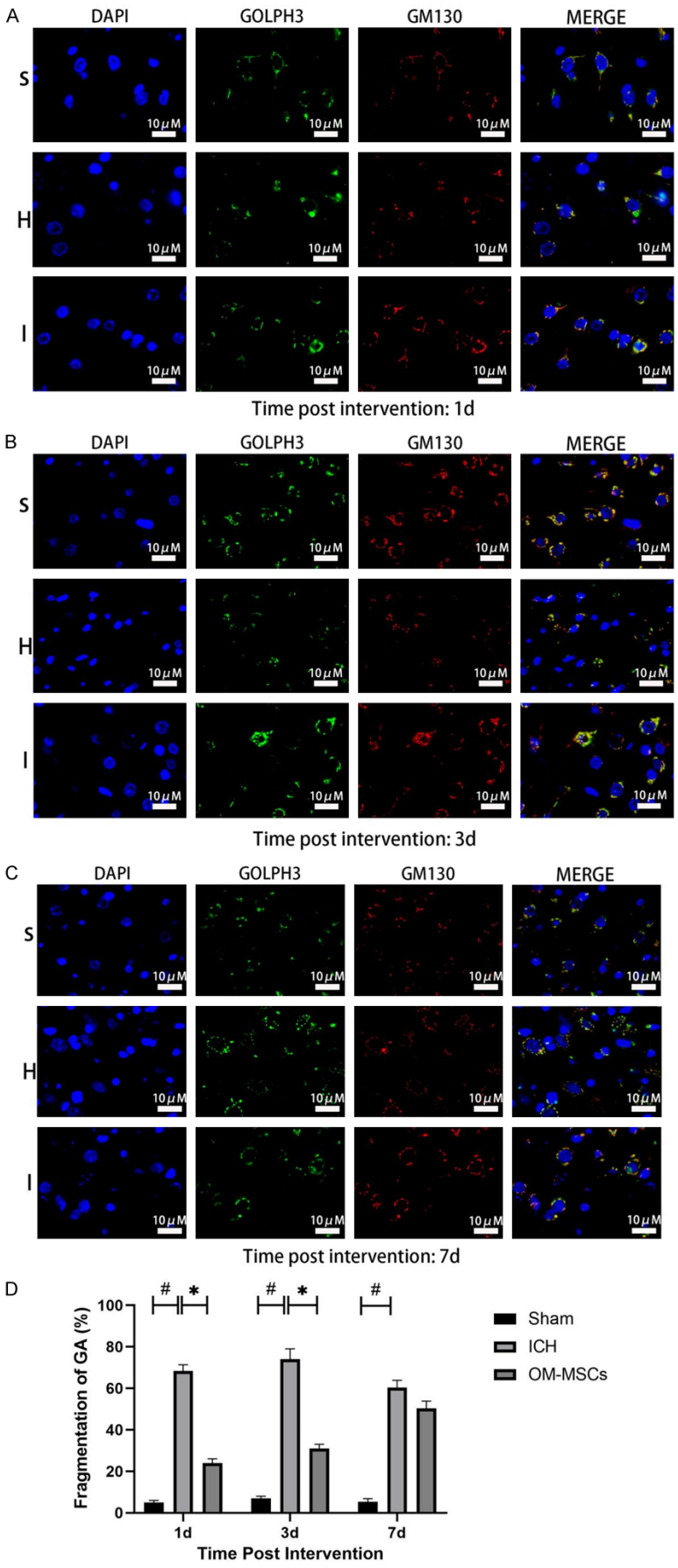

Figure 4. Immunofluorescence 1 d (A), 3 d (B), 7 d (C) after intervention (×1000) and (D) Quantitation (mean ± SEM) of (A-C) from three independent experiments. GA exhibited significant fragmentation in ICH group in comparison with sham operation group on 1 d, 3 d and 7 d. Remarkably, structure of GA in OM-MSCs intervention group was visibly maintained and GA fragmentation was distinctly reduced compared with ICH group on 1 d and 3 d. S: sham operation group, H: ICH group, I: OM-MSCs intervention group, same as below. #P < 0.05 ICH versus Sham, *P < 0.05 OM-MSCs versus ICH.

more suitable for large-scale clinical trials. However, this method has drawbacks that significantly limit its effectiveness. For instance, transplanted cells can disperse throughout the entire body, including the liver and lungs. Additionally, the presence of the blood-brain barrier increases the required dosage of transplanted cells, consequently elevating the risk of potential hepatotoxicity and pulmonary embolism. Therefore, while intravenous transplantation offers ease and accessibility, its limitations highlight the need for further study and improvement. The most effective method for behavioral and structural recovery after ICH, as revealed by a meta regression analysis involving 40 studies and 1021 animal models, is intracerebral transplantation [52]. This technique offers the advantage of accurate positioning, leading to reduced cell loss and minimized migration distance in vivo. Consequently, it allows for a decrease in cell dose. However, its drawbacks include trauma and the formation of cell clusters, which hinder further proliferation and migration. In a

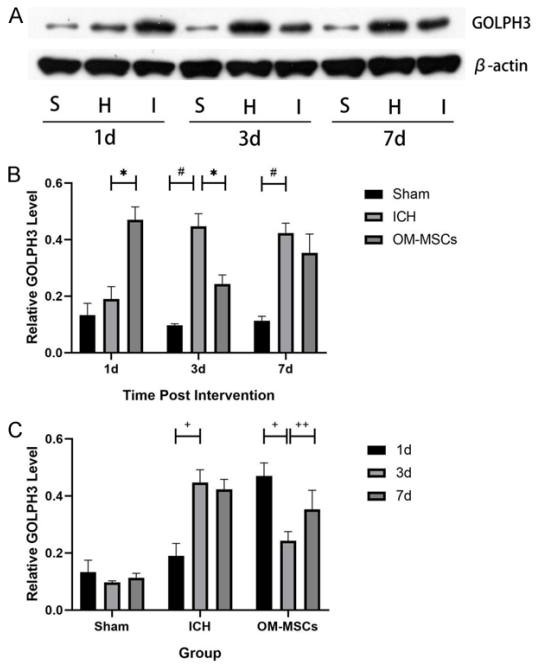

Figure 5. Expression level of GOLPH3 in three groups at different time points. Expression of GOLPH3 was significantly upregulated after ICH on 3 d, 7 d compared with Sham group. OM-MSCs administration remarkably inhibited ICH-induced upregulation of GOLPH3 at 3rd day. S or Sham: sham operation group, H or ICH: ICH group, I or OM-MSCs: OM-MSCs intervention group. #P < 0.05 ICH versus Sham, *P < 0.05 OM-MSCs versus ICH, +P < 0.05 1 d versus 3 d, ++P < 0.05 3 d versus 7 d.

study by Zhang Q et al., it was demonstrated that umbilical cord MSCs intracerebral transplantation, combined with minimally invasive hematoma aspiration, exhibited superior efficacy compared to the two therapies alone [53]. Building on this finding, intracerebral administration is adopted in our study, as we believe that intracerebral transplantation of OM-MSCs holds significant clinical value. Furthermore, we propose that OM-MSCs intracerebral transplantation, in combination with minimally invasive surgery for ICH, may emerge as an effective alternative therapy in the future. The optimal standard for the dose of transplanted cells largely depends on the route of transplantation, which warrants further research. Generally, there exists a 'threshold dose' refers to the minimum number of cells required to achieve the expected effects, while the 'ceiling dose' represents the maximum number of cells that will not further increase therapeutic effects, and may instead lead to adverse consequences such as embolization, organ toxicity, and tumorigenesis. Previous studies have predominantly utilized million-grade cells to treat ICH, yielding acceptable results [45]. Empirically, 1×10^6 cells have been used with safe and effective outcomes. However, no comparative analysis of different doses has been conducted.

In the initial phase of our investigation, we explored the ability of OM-MSCs to reduce apoptosis following experimental ICH in rats. This direction of inquiry was motivated by a prior study which revealed the potential of adipose-derived mesenchymal stem cells to mitigate nervous tissue injury and decrease cell apoptosis in ICH [54]. Additionally, Yoji Kuramoto et al. proposed that the administration of human amnion-derived stem cells during the acute phase could alleviate neurobehavioral deficits associated with intracerebral hemorrhage by suppressing local inflammation and apoptosis [55]. These findings provided a foundation for our exploration of the impact of OM-MSCs on apoptosis in the context of ICH. Under fluorescence microscope, a small number of TUNEL staining (green) positive cells were observed in sham operation group and there was no significant change over time (P > 0.05), which was consistent with physiological apoptosis in normal (or minor trauma) brain tissue. Compared with sham operation group, ICH group showed a significant increase in TUNEL positive cells and apoptosis rate on 3 d (P < 0.05), indicating that the GAS-induced apoptosis occurred not only after oxyglucose deprivation/reperfusion [12], but also after ICH. Following the transplantation of OM-MSCs at the same time point, OM-MSCs intervention group exhibited a significant reduction in TUNEL positive cells and apoptosis rate compared with ICH group (P < 0.05), suggesting that the early administration of OM-MSCs could significantly inhibit GAS-induced apoptosis, and then alleviate secondary brain injury. This result aligned with findings reported in the literature [55, 56]. It is worth noting that expression of GOLPH3 in OM-MSCs intervention group was significantly higher than that in ICH group on day 1 (P < 0.05), while apoptosis rate was significantly lower than that in ICH group (P < 0.05); on day 7, expression of GOLPH3 in ICH group was significantly higher than that in sham operation group (P < 0.05), but there was no significant difference in apoptosis rate (P > 0.05). These results indicate a lack of complete consistency between the intracellular stress

level and tissue stress level at 1 day and 7 days post-ICH, suggesting potential involvement of other mechanisms such as stress-related autophagy [57, 58] or inflammation [59] which still need to be elucidated by further experiments.

In the second part of our study, we investigated the potential of OM-MSCs in mitigating GA fragmentation and suppressing the expression of GOLPH3 subsequent to experimental ICH in rats. Previous research has demonstrated the capacity of OM-MSCs to alleviate the Golgi apparatus stress response in cases of cerebral ischemia/reperfusion injury through the PEDF-PI3K/Akt/mTOR signaling pathway [60]. Based on the experimental results, at different time points (1 d, 3 d, and 7 d), the expression of GOLPH3 in the sham operation group was consistently low and showed no significant differences ($P > 0.05$). This finding aligns with the typical low level of GOLPH3 expression in physiological conditions or minor trauma, which helps maintain the normal morphology and physiological function of the Golgi apparatus (GA). On the first day after ICH, the expression of GOLPH3 in the ICH group appeared to be higher than that in the sham operation group, but the variance was not statistically significant ($P > 0.05$). However, on days 3 and 7, the expression of GOLPH3 in the ICH group was notably higher than that in the sham operation group ($P < 0.05$), indicating a significant increase. Notably, there was no significant difference between the expression levels in the ICH group on days 3 and 7 ($P > 0.05$), suggesting that the expression of GOLPH3 gradually increased in the first three days after ICH, and then stabilized at a higher level in the following 3-7 days. The observation of obvious GA fragmentation in 1 d, 3 d, and 7 d ICH group through immunofluorescence confocal examination of GOLPH3 and GM130 suggests the involvement of GOLPH3 in regulating protein expression during secondary brain injury following ICH and leading to morphological fragmentation. This finding indicates that GOLPH3 participates in GAS by up-regulating protein expression. These results are in line with previously reported findings in a cerebral ischemia/reperfusion model [60]. The expression of GOLPH3 in the 3 d OM-MSCs intervention group was found to be significantly lower than that in the 3 d ICH group ($P < 0.05$) post-intervention. Subsequent immunofluorescence confocal observation of GOLPH3 and GM130 revealed a significant reduction in GA fragmentation in both the 1 d and 3 d OM-MSCs groups. These findings indicate that early administration of OM-MSCs effectively decreased GOLPH3 protein expression, inhibited GA fragmentation, and therefore mitigated the progression of GAS. Consequently, it can be inferred that OM-MSCs have the potential to alleviate GAS in both ischemic and hemorrhagic stroke models. However, it should also be noted that expression of GOLPH3 in OM-MSCs group was further increased compared with ICH group after 1 day of intervention, and this difference was found to be statistically significant ($P < 0.05$). We attribute this finding to the strong inflammatory reaction of the tissue surrounding the hematoma in the ICH rats on day 1, which had a significant adverse impact on the activity and function of the transplanted OM-MSCs. This hostile microenvironment presented formidable challenges to the survival and proliferation of the stem cells, resulting in a substantial number of dead transplanted cells and creating an increased space-occupying effect, consequently elevating the stress level in the tissues and cells. Additionally, the up-regulated expression of GOLPH3 may have been generated by the partial transplanted cells experiencing ischemia, hypoxia or even death. Subsequently, after 7 days of intervention, there appeared to be seemingly lower expression of GOLPH3 and GA fragmentation in the OM-MSCs intervention group compared to the ICH group, however, this difference was not statistically significant ($P > 0.05$). At this juncture, the expression of GOLPH3 in the ICH group remained high, indicating the weakened antioxidant stress effect of the OM-MSCs after 7 days of transplantation. Notably, it is well established in the literature that the secondary brain injury after ICH mainly occurs within 1 week [45]. Beyond this point, the surviving OM-MSCs primarily transform into neurons and glial cells for replacement, aligning with the characteristic “early anti-inflammatory effect, mid-late replacement role” mechanism of mesenchymal stem cells [61].

Our study also has several limitations that need to be taken into account. Firstly, it is important to extend the observation period to include additional time points such as 15 days, 1

month, and 3 months, in order to provide a more comprehensive understanding of the long-term neuroprotective effects of OM-MSCs on both histological and functional recovery. Furthermore, to validate GA fragmentation, more distinct images can be obtained using advanced techniques such as electron microscopy. Additionally, it is worth noting that there is increasing evidence supporting the notion that the paracrine effects of transplanted MSCs are likely the primary mechanism through which neuroprotective effects are exerted. MSC-derived extracellular vesicles, which are believed to transport functional molecules such as proteins and microRNAs to neuron or glial cells, have been shown to exhibit potent protective effects in ICH. Therefore, in future research, it will be important to investigate the potential effects of OM-MSCs-derived extracellular vesicles on the Golgi apparatus and the underlying mechanisms in the context of ICH.

Conclusion

In summary, our study demonstrated that the rate of apoptosis, fragmentation of GA, and expression of GOLPH3 exhibited significant increases following ICH in SD rats. Conversely, all of these factors demonstrated significant decreases subsequent to early intervention with OM-MSCs, thereby exerting neuroprotective effects. Although more work is required, current data shed new light on the treatment of ICH, suggesting that OM-MSCs therapy could be a novel therapeutic strategy applicable for ICH.

Acknowledgements

This work was supported by the National Natural Science Foundation of China (grant numbers 82271367 and 82101544); Natural Science Foundation of Hunan Province, China (grant number 2023JJ30331); and Key Project of Hunan Provincial Maternal and Child Health Care Hospital (grant number 2021RX01).

Disclosure of conflict of interest

None.

Address correspondence to: Dezhen Peng, Clinical Nursing Teaching and Research Section, The Second Xiangya Hospital of Central South University, No. 139 Renmin Road, Changsha 410011, Hunan, The People's Republic of China. Tel: +86-15675119181; E-mail: pengdz6601@csu.edu.cn

References

[1] Feigin VL, Lawes CM, Bennett DA, Barker-Collo SL and Parag V. Worldwide stroke incidence and early case fatality reported in 56 population-based studies: a systematic review. Lancet Neurol 2009; 8: 355-369.
[2] Magid-Bernstein J, Girard R, Polster S, Srinath A, Romanos S, Awad IA and Sansing LH. Cerebral hemorrhage: pathophysiology, treatment, and future directions. Circ Res 2022; 130: 1204-1229.
[3] Campbell BCV and Khatri P. Stroke. Lancet 2020; 396: 129-142.
[4] Gross BA, Jankowitz BT and Friedlander RM. Cerebral intraparenchymal hemorrhage: a review. JAMA 2019; 321: 1295-1303.
[5] Sheth KN. Spontaneous intracerebral hemorrhage. N Engl J Med 2022; 387: 1589-1596.
[6] Aronowski J and Zhao X. Molecular pathophysiology of cerebral hemorrhage: secondary brain injury. Stroke 2011; 42: 1781-1786.
[7] Keep RF, Hua Y and Xi G. Intracerebral haemorrhage: mechanisms of injury and therapeutic targets. Lancet Neurol 2012; 11: 720-731.
[8] Shi K, Tian DC, Li ZG, Ducruet AF, Lawton MT and Shi FD. Global brain inflammation in stroke. Lancet Neurol 2019; 18: 1058-1066.
[9] Kummer E and Ban N. Mechanisms and regulation of protein synthesis in mitochondria. Nat Rev Mol Cell Biol 2021; 22: 307-325.
[10] Ott M, Gogvadze V, Orrenius S and Zhivotovsky B. Mitochondria, oxidative stress and cell death. Apoptosis 2007; 12: 913-922.
[11] Jiang Z, Hu Z, Zeng L, Lu W, Zhang H, Li T and Xiao H. The role of the Golgi apparatus in oxidative stress: is this organelle less significant than mitochondria? Free Radic Biol Med 2011; 50: 907-917.
[12] Li T, You H, Mo X, He W, Tang X, Jiang Z, Chen S, Chen Y, Zhang J and Hu Z. GOLPH3 mediated Golgi stress response in modulating N2A cell death upon Oxygen-Glucose deprivation and reoxygenation injury. Mol Neurobiol 2016; 53: 1377-1385.
[13] Li T, You H, Zhang J, Mo X, He W, Chen Y, Tang X, Jiang Z, Tu R, Zeng L, Lu W and Hu Z. Study of GOLPH3: a potential stress-inducible protein from Golgi apparatus. Mol Neurobiol 2014; 49: 1449-1459.
[14] Al-Kawaz MN, Hanley DF and Ziai W. Advances in therapeutic approaches for spontaneous intracerebral hemorrhage. Neurotherapeutics 2020; 17: 1757-1767.
[15] Haller JT, Wiss AL, May CC, Jones GM and Smetana KS. Acute management of hyperten-

sion following intracerebral hemorrhage. Crit Care Nurs Q 2019; 42: 129-147.
[16] Fogarty Mack P. Intracranial haemorrhage: therapeutic interventions and anaesthetic management. Br J Anaesth 2014; 113 Suppl 2: ii17-25.
[17] Hemphill JC 3rd, Greenberg SM, Anderson CS, Becker K, Bendok BR, Cushman M, Fung GL, Goldstein JN, Macdonald RL, Mitchell PH, Scott PA, Selim MH and Woo D; American Heart Association Stroke Council; Council on Cardiovascular and Stroke Nursing; Council on Clinical Cardiology. Guidelines for the management of spontaneous intracerebral hemorrhage: a guideline for healthcare professionals from the American Heart Association/American Stroke Association. Stroke 2015; 46: 2032-2060.
[18] Dowlatshahi D, Demchuk AM, Flaherty ML, Ali M, Lyden PL and Smith EE; VISTA Collaboration. Defining hematoma expansion in intracerebral hemorrhage: relationship with patient outcomes. Neurology 2011; 76: 1238-1244.
[19] Vinukonda G, Liao Y, Hu F, Ivanova L, Purohit D, Finkel DA, Giri P, Bapatla L, Shah S, Zia MT, Hussein K, Cairo MS and La Gamma EF. Human cord blood-derived unrestricted somatic stem cell infusion improves neurobehavioral outcome in a rabbit model of intraventricular hemorrhage. Stem Cells Transl Med 2019; 8: 1157-1169.
[20] Xun C, Ge L, Tang F, Wang L, Zhuo Y, Long L, Qi J, Hu L, Duan D, Chen P and Lu M. Insight into the proteomic profiling of exosomes secreted by human OM-MSCs reveals a new potential therapy. Biomed Pharmacother 2020; 131: 110584.
[21] Ranganath SH, Levy O, Inamdar MS and Karp JM. Harnessing the mesenchymal stem cell secretome for the treatment of cardiovascular disease. Cell Stem Cell 2012; 10: 244-258.
[22] Ge L, Jiang M, Duan D, Wang Z, Qi L, Teng X, Zhao Z, Wang L, Zhuo Y, Chen P, He X and Lu M. Secretome of olfactory mucosa mesenchymal stem cell, a multiple potential stem cell. Stem Cells Int 2016; 2016: 1243659.
[23] Rosado-De-Castro PH, de Carvalho FG, de Freitas GR, Mendez-Otero R and Pimentel-Coelho PM. Review of preclinical and clinical studies of bone marrow-derived cell therapies for intracerebral hemorrhage. Stem Cells Int 2016; 2016: 4617983.
[24] Delorme B, Nivet E, Gaillard J, Haupl T, Ringe J, Deveze A, Magnan J, Sohier J, Khrestchatisky M, Roman FS, Charbord P, Sensebe L, Layrolle P and Feron F. The human nose harbors a niche of olfactory ectomesenchymal stem cells displaying neurogenic and osteogenic properties. Stem Cells Dev 2010; 19: 853-866.
[25] Huard JM, Youngentob SL, Goldstein BJ, Luskin MB and Schwob JE. Adult olfactory epithelium contains multipotent progenitors that give rise to neurons and non-neural cells. J Comp Neurol 1998; 400: 469-486.
[26] Lindsay SL, Johnstone SA, Mountford JC, Sheikh S, Allan DB, Clark L and Barnett SC. Human mesenchymal stem cells isolated from olfactory biopsies but not bone enhance CNS myelination in vitro. Glia 2013; 61: 368-382.
[27] Ge L, Duan D, Wang L, Zhao Z, Teng X and Lu M. Culture, identification and biological characteristics of human olfactory mucosa mesenchymal stem cells (in Chinses). J Hunan Normal Univ (Med Sci) 2015; 12: 7-10.
[28] Ge L and Lu M. Research progress of olfactory mucosal mesenchymal stem cells in nerve repair (in Chinese). Journal of International Neurology and Neurosurgery 2014; 41: 66-69.
[29] Duan D and Lu M. Olfactory mucosa: a rich source of cell therapy for central nervous system repair. Rev Neurosci 2015; 26: 281-293.
[30] Ge L, Zhuo Y, Duan D, Zhao Z, Teng X, Wang L and Lu M. Biological characteristics of human olfactory mucosa mesenchymal stem cells. Zhong Nan Da Xue Xue Bao Yi Xue Ban 2015; 40: 53-58.
[31] Rosenberg GA, Mun-Bryce S, Wesley M and Kornfeld M. Collagenase-induced intracerebral hemorrhage in rats. Stroke 1990; 21: 801-807.
[32] Hua W, Ma S, Pang Y, Liu Q, Wang Y, Liu Z, Zhao N, Ren N, Jin S, Wang B, Song Y and Qi J. Intracerebral Hemorrhage-Induced brain injury: the role of lysosomal-associated transmembrane protein 5. Mol Neurobiol 2023; 60: 7060-7079.
[33] Longa EZ, Weinstein PR, Carlson S and Cummins R. Reversible middle cerebral artery occlusion without craniectomy in rats. Stroke 1989; 20: 84-91.
[34] Xie J, Wang B, Wang L, Dong F, Bai G and Liu Y. Intracerebral and intravenous transplantation represents a favorable approach for application of human umbilical cord mesenchymal stromal cells in intracerebral hemorrhage rats. Med Sci Monit 2016; 22: 3552-3561.
[35] Yabuno S, Yasuhara T, Nagase T, Kawauchi S, Sugahara C, Okazaki Y, Hosomoto K, Sasada S, Sasaki T, Tajiri N, Borlongan CV and Date I. Synergistic therapeutic effects of intracerebral transplantation of human modified bone marrow-derived stromal cells (SB623) and voluntary exercise with running wheel in a rat model of ischemic stroke. Stem Cell Res Ther 2023; 14: 10.
[36] Chen M, Li X, Zhang X, He X, Lai L, Liu Y, Zhu G, Li W, Li H, Fang Q, Wang Z and Duan C. The inhibitory effect of mesenchymal stem cell on blood-brain barrier disruption following intracerebral hemorrhage in rats: contribution of TSG-6. J Neuroinflammation 2015; 12: 61.

[37] Liu J, He J, Huang Y, Ge L, Xiao H, Zeng L, Jiang Z, Lu M and Hu Z. Hypoxia-preconditioned mesenchymal stem cells attenuate microglial pyroptosis after intracerebral hemorrhage. Ann Transl Med 2021; 9: 1362.
[38] Joshi G, Chi Y, Huang Z and Wang Y. Abeta-induced Golgi fragmentation in Alzheimer's disease enhances Abeta production. Proc Natl Acad Sci U S A 2014; 111: E1230-E1239.
[39] Zhang J, Tan J, Hu Z, Chen C and Zeng L. HDAC6 inhibition protects against OGDR-induced Golgi fragmentation and apoptosis. Oxid Med Cell Longev 2019; 2019: 6507537.
[40] Cui C, Cui Y, Gao J, Li R, Jiang X, Tian Y, Wang K and Cui J. Intraparenchymal treatment with bone marrow mesenchymal stem cell-conditioned medium exerts neuroprotection following intracerebral hemorrhage. Mol Med Rep 2017; 15: 2374-2382.
[41] Wang D and Li Y. The mechanisms of mesenchymal stem cell transplantation therapy (in Chinese). Translational Medicine Journal 2019; 8: 257-261.
[42] Seyfried DM, Han Y, Yang D, Ding J, Shen LH, Savant-Bhonsale S and Chopp M. Localization of bone marrow stromal cells to the injury site after intracerebral hemorrhage in rats. J Neurosurg 2010; 112: 329-335.
[43] Otero L, Zurita M, Bonilla C, Aguayo C, Rico MA, Rodriguez A and Vaquero J. Allogeneic bone marrow stromal cell transplantation after cerebral hemorrhage achieves cell transdifferentiation and modulates endogenous neurogenesis. Cytotherapy 2012; 14: 34-44.
[44] Chen X, Shi Z, Zhu Q, Cha Z, Luo B, Fang Q and Yin G. Proliferaiton and differenitation of neural stem cells in hemorrhagic cerebrospinal fluid (in Chinese). Journal of Clinical Neurosurgery 2011; 8: 269-271.
[45] Gong C, Boulis N, Qian J, Turner DE, Hoff JT and Keep RF. Intracerebral hemorrhage-induced neuronal death. Neurosurgery 2001; 48: 875-882; discussion 882-883.
[46] Geng W, He X and Wu Q. The therapeutic effect of bone marrow mesenchymal stem cell transplantation on intracerebral hemorrhage in rats (in Chinses). Journal of Xinjiang Medical University 2018; 41: 861-864.
[47] Kuramoto Y, Takagi T, Tatebayashi K, Beppu M, Doe N, Fujita M and Yoshimura S. Intravenous administration of human adipose-derived stem cells ameliorates motor and cognitive function for intracerebral hemorrhage mouse model. Brain Res 2019; 1711: 58-67.
[48] Cui LL, Kerkela E, Bakreen A, Nitzsche F, Andrzejewska A, Nowakowski A, Janowski M, Walczak P, Boltze J, Lukomska B and Jolkkonen J. The cerebral embolism evoked by intra-arterial delivery of allogeneic bone marrow mesenchymal stem cells in rats is related to cell dose and infusion velocity. Stem Cell Res Ther 2015; 6: 11.
[49] Sun J, Wei ZZ, Gu X, Zhang JY, Zhang Y, Li J and Wei L. Intranasal delivery of hypoxia-preconditioned bone marrow-derived mesenchymal stem cells enhanced regenerative effects after intracerebral hemorrhagic stroke in mice. Exp Neurol 2015; 272: 78-87.
[50] Ahn SY, Chang YS, Sung DK, Sung SI, Yoo HS, Lee JH, Oh WI and Park WS. Mesenchymal stem cells prevent hydrocephalus after severe intraventricular hemorrhage. Stroke 2013; 44: 497-504.
[51] Chen L, Xi H, Huang H, Zhang F, Liu Y, Chen D and Xiao J. Multiple cell transplantation based on an intraparenchymal approach for patients with chronic phase stroke. Cell Transplant 2013; 22 Suppl 1: S83-S91.
[52] Hu Y, Liu N, Zhang P, Pan C, Zhang Y, Tang Y, Deng H, Aimaiti M, Zhang Y, Zhou H, Wu G and Tang Z. Preclinical studies of stem cell transplantation in intracerebral hemorrhage: a systemic review and meta-analysis. Mol Neurobiol 2016; 53: 5269-5277.
[53] Zhang Q, Shang X, Hao M, Zheng M, Li Y, Liang Z, Cui Y and Liu Z. Effects of human umbilical cord mesenchymal stem cell transplantation combined with minimally invasive hematoma aspiration on intracerebral hemorrhage in rats. Am J Transl Res 2015; 7: 2176-2186.
[54] Zhang Y, Deng H, Hu Y, Pan C, Wu G, Li Q and Tang Z. Adipose-derived mesenchymal stem cells stereotactic transplantation alleviate brain edema from intracerebral hemorrhage. J Cell Biochem 2019; 120: 14372-14382.
[55] Kuramoto Y, Fujita M, Takagi T, Takeda Y, Doe N, Yamahara K and Yoshimura S. Early-phase administration of human amnion-derived stem cells ameliorates neurobehavioral deficits of intracerebral hemorrhage by suppressing local inflammation and apoptosis. J Neuroinflammation 2022; 19: 48.
[56] Ding H, Jia Y, Lv H, Chang W, Liu F and Wang D. Extracellular vesicles derived from bone marrow mesenchymal stem cells alleviate neuroinflammation after diabetic intracerebral hemorrhage via the miR-183-5p/PDCD4/NLRP3 pathway. J Endocrinol Invest 2021; 44: 2685-2698.
[57] Zhang X, Wang L, Ireland SC, Ahat E, Li J, Bekier ME 2nd, Zhang Z and Wang Y. GORASP2/GRASP55 collaborates with the PtdIns3K UVRAG complex to facilitate autophagosome-lysosome fusion. Autophagy 2019; 15: 1787-1800.
[58] Gosavi P, Houghton FJ, Mcmillan PJ, Hanssen E and Gleeson PA. The Golgi ribbon in mammalian cells negatively regulates autophagy by modulating mTOR activity. J Cell Sci 2018; 131: jcs211987.

[59] Chen L, Sun X, Xiao H, Xu F, Yang Y, Lin Z, Chen Z, Quan S and Huang H. PAQR3 regulates phosphorylation of FoxO1 in insulin-resistant HepG2 cells via NF-kappaB signaling pathway. Exp Cell Res 2019; 381: 301-310.
[60] He J, Liu J, Huang Y, Tang X, Xiao H, Liu Z, Jiang Z, Zeng L, Hu Z and Lu M. OM-MSCs alleviate the Golgi apparatus stress response following cerebral ischemia/reperfusion injury via the PEDF-PI3K/Akt/mTOR signaling pathway. Oxid Med Cell Longev 2021; 2021: 4805040.
[61] Andres RH, Guzman R, Ducray AD, Mordasini P, Gera A, Barth A, Widmer HR and Steinberg GK. Cell replacement therapy for intracerebral hemorrhage. Neurosurg Focus 2008; 24: E16.